

Magnetic Circular Dichroism near the Fermi Level

Takeshi Nakagawa and Toshihiko Yokoyama*

*Department of Molecular Structure, Institute for Molecular Science, and Department of Structural Molecular Science,
The Graduate University for Advanced Studies (Sokendai), Myodaiji-cho, Okazaki, 444-8585, Japan*

(Received 30 January 2006; published 12 June 2006)

We report the observation of enhanced magnetic circular dichroism (MCD) near the Fermi level using visible and ultraviolet lasers. More than 10% MCD asymmetry is achieved for a perpendicularly magnetized 12 ML (monolayer) Ni film on Cu(001). By changing the work function with the aid of cesium adsorption, the MCD asymmetry of Ni(12 ML)/Cu(001) is found to be enhanced only near the photoemission threshold and to drop down to 0.1% at the photon energy larger than the work function by 0.6 eV. A theoretical calculation also shows enhanced MCD near the photoemission threshold, qualitatively in agreement with the experimental results. Other ultrathin films of 6 ML Ni, 15 ML Co, and 3 and 15 ML Fe on Cu(001) are also investigated. It is found that the perpendicularly magnetized films show much larger MCD asymmetries than the in-plane magnetized films as in the Kerr effect.

DOI: [10.1103/PhysRevLett.96.237402](https://doi.org/10.1103/PhysRevLett.96.237402)

PACS numbers: 78.20.Ls, 73.61.-r, 75.70.-i, 79.60.-i

Owing to recent developments of synchrotron radiation and lasers, photon probe techniques are now indispensable to the study of surface and thin film magnetism. Magnetic circular dichroism (MCD) nowadays prevails, which measures average magnetization in the presence of the spin-orbit coupling (SOC). X-ray magnetic circular dichroism (XMCD) [1] has attracted extensive interest since it allows element specific measurements and gives the absolute values of spin and orbital magnetic moments using the sum rules [2,3]. The XMCD asymmetry is quite large because of the strong SOC in the core shell. Two-dimensional imaging of magnetic materials based on the XMCD technique is now available using third generation synchrotron light sources together with photoelectron emission microscopy (PEEM) [4]. Its spatial resolution achieves ~ 10 nm, while the time resolution is limited to ~ 70 ps due to the pulse width of the synchrotron radiation itself [5].

The MCD in the regions from infrared to ultraviolet (UV) is also a useful tool. The magneto-optical Kerr effect (MOKE) detects the rotation and distortion of the polarization of reflected light from magnetic materials [6,7]. The Kerr effect in the valence bands of ultrathin films usually rotates the polarization and changes the ellipticity only by 10^{-2} – 10^{-6} rad because of much weaker SOC in the valence shells. In valence band photoemission, nevertheless, extensive sophisticated works have been performed using circularly polarized synchrotron radiation and an angle-resolved spectrometer [8–10]. They have shown that the MCD asymmetry is high enough to be measured (sometimes $\sim 30\%$ particularly near the Fermi level). Normal photoemission is, however, essential for the large MCD asymmetry. Angle integrated experiments have been believed to degrade the asymmetry, although they are crucial to spatiotemporal measurements. Marx *et al.* [11] have investigated magnetic linear dichroism (MLD) using PEEM with a Hg lamp. They observed 0.37% dichroism on

a 100 nm Fe film, which is comparable to the asymmetry of the transverse Kerr effect and is 1–2 orders of magnitude smaller than typical XMCD asymmetries. In spite of its small MCD asymmetry, UV light offers the possibility to obtain a substantially higher spatiotemporal resolution.

In this Letter, we show large MCD near the Fermi level induced by UV and visible lasers. The obtained MCD asymmetry is as much as 10%–12% for a 12 ML (monolayer) Ni film. It is found that the MCD asymmetry is noticeably enhanced only near the photoemission threshold and is suppressed quickly as the photon energy becomes larger than the work function. The enhanced MCD asymmetry can also be explained by a theoretical calculation.

Experiments were performed in an ultrahigh vacuum chamber with a base pressure of $<4 \times 10^{-10}$ Torr. Ultrathin films of Fe, Ni, and Co were prepared at 300 K on Cu(001) surfaces that were cleaned by Ar^+ sputtering and subsequent annealing at 825 K. To change the sample work functions, Cs was deposited from commercial dispensers at a rate of 0.001–0.01 ML/min. The emitted photocurrent was measured via the drain current from the sample by placing an anode plate (2 kV) in front of the sample. An electromagnet with a maximum magnetic field of 2500 Oe was used to measure the MCD asymmetry and the magnetization hysteresis curves. A laser diode (635 nm, 1.95 eV, 5 mW) and a HeCd laser (325 nm, 3.81 eV, 10 mW) were used as exciting sources, which provide $\sim 10^{16}$ photons/s. Their polarizations (up to 100% circular polarization) were controlled by phase compensators (quarter wave plates). In order to determine the work function Φ of the sample, the cutoff energy of the secondary electrons was measured using a retarding field analyzer and an electron gun. The accuracy of the work function was around ± 0.1 eV. For more accurate determination of the work function near the threshold ($h\nu - \Phi < 0.15$ eV, where $h\nu$ is the photon energy), the experimentally ob-

tained photoemission yield as a function of the Cs amount was fitted with the Fermi distribution function by assuming that the density of states is constant and the work function changes linearly with the deposition time in this narrow energy range. This method allows us to calibrate the work function with the accuracy of ± 0.01 eV near the threshold.

In order to verify the experimental observations at least qualitatively, a simple band structure calculation using WIEN2K [12] was performed for bulk fcc Ni. The SOC was included within the second variational approach [13]. A linear-response formalism was employed to compute the optical conductivity within the dipolar approximation [14]. For the evaluation of photoemission yields, only the transitions above the vacuum level were taken into account. The MCD asymmetry is then given as the ratio between the imaginary part of the off-diagonal element and the real part of the diagonal element. Although the process of photoemission from a solid surface should be taken into account in order to compare the calculation with the experiment directly, the present calculation should be meaningful for qualitative estimation of the MCD asymmetry near the threshold.

Figure 1(a) shows the magnetization hysteresis (M - H) curves obtained on Cs/Ni(12 ML)/Cu(001) together with the MOKE result. The photon energy used was 1.95 eV. The MCD and MOKE measurements were performed in a polar configuration since the Ni film has a perpendicular magnetization easy axis [15]. The shape of the M - H curve obtained by MCD is almost identical to that obtained by MOKE, indicating that the MCD correctly detects the magnetization process. Figure 1(b) shows the MCD asymmetry as a function of the azimuthal angle of the quarter wave plate. The asymmetry is perfectly fitted with the cosine function. The cosine dependence verifies that the angular momentum delivered by the photon polarization gives rise to the MCD.

Figure 1(c) shows results of the MCD asymmetry using the photon energies of 3.81 and 1.95 eV in successive experiments on the same sample. The work function was changed by Cs adsorption. Here, the MCD asymmetry A is defined as $A = (I^{\text{left}} - I^{\text{right}})/(I^{\text{left}} + I^{\text{right}})$, where I^{left} and I^{right} are the drain currents with left- and right-circularly polarized lights, respectively. The horizontal scale represents the maximum kinetic energy of the photoelectrons, the photon energy $h\nu$ subtracted by the work function Φ . The drain current, I^{left} or I^{right} , at the energy of $h\nu - \Phi$ corresponds to the integrated photoemission yield in the energy range between $E_F + \Phi - h\nu$ and E_F (E_F the Fermi level).

The most striking result in Fig. 1(c) is that the obtained MCD asymmetry is as much as 10%–12% near the photoemission threshold and is suppressed quickly as the energy $h\nu - \Phi$ becomes larger. The abrupt reduction of the MCD asymmetry against Cs deposition does not stem from the deterioration of the surface due to Cs. This is

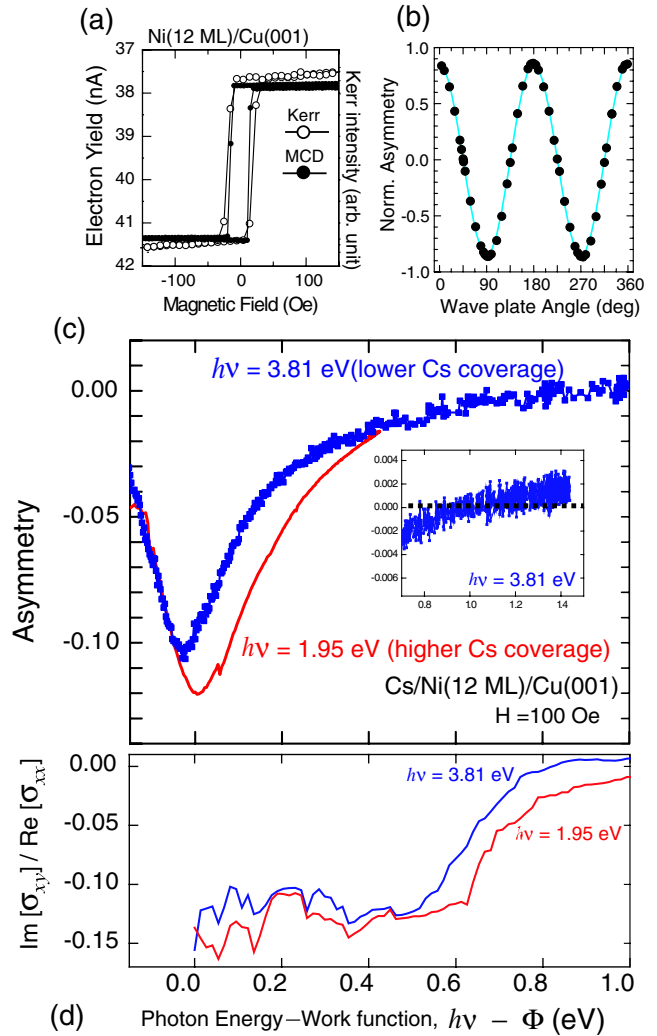


FIG. 1 (color online). (a) Magnetization curves of a Cs/Ni(12 ML)/Cu(001) in a polar configuration with photoemission MCD (filled circles) and MOKE measurements (open circles). The incident angle of the light with respect to surface normal is 45° in both cases. (b) Dependence of the MCD asymmetry on the azimuthal angle of the quarter wave plate. The light incidence angle was 45° . The solid line is a cosine curve fit. (c) MCD asymmetry from Cs/Ni(12 ML)/Cu(001) at normal incidence. The inset shows the magnified plot of the asymmetry for a lower work function, exhibiting inversion of the sign. (d) Calculated MCD asymmetry of bulk fcc Ni ($a_0 = 0.361$ nm) by WIEN2K.

evidenced by the two different experiments using the 1.95 and 3.81 eV lasers. In spite that for the 1.95 and 3.81 eV laser experiments the Cs amounts were about 1 order of magnitude different around the threshold energy (~ 0.15 and ~ 0.03 ML, respectively), the MCD asymmetry curves are almost identical to each other. The calculated results in Fig. 1(d) also exhibit enhanced asymmetries near the Fermi level, which do not significantly depend on the excitation energies. It is also noted that in the vicinity of $h\nu - \Phi \sim 1$ (eV) the MCD asymmetry [see the inset of Fig. 1(c)]

changes its sign from negative to positive. This also agrees with the calculated spectra in Fig. 1(d).

The orientation of the magnetization axis has a drastic effect on the MCD asymmetry. Figure 2 shows the MCD result as a function of the Ni thickness on a wedge Ni sample, where a spin reorientation transition (SRT) occurs around 8 ML. The MCD asymmetry drastically changes across the spin reorientation transition. The in-plane magnetized films show roughly 1 order of magnitude smaller asymmetry than that in perpendicularly magnetized ones, although the M - H curve by the MCD is clearly observed for the 6 ML Ni film (see the inset of Fig. 2). Such a drastic variation is usually observed in the rotation or ellipticity of MOKE, where the reduction scale is estimated as ~ 10 at $h\nu = 1.95$ eV [16]. Although the SOC significantly contributes to the SRT, the difference of the orbital magnetic moment on the SRT between the in plane and the out of plane is at most twice [17]. Therefore, the effect of the SOC is not dominant. The principal reason for such drastic differences in MCD and MOKE between the polar and longitudinal configurations should be the reflection of the light. For visible and UV light, total reflection occurs, and the sign of the photon helicity is changing along the in-plane direction and does not change along the surface normal. This leads to the compensation (enhancement) of the MCD or MOKE signals in in-plane (perpendicularly) magnetized films. This is not the case for the XMCD because the x rays do not reflect, and hence the XMCD signal can equally be observable irrespective of the magnetization direction of the sample. The present MCD com-

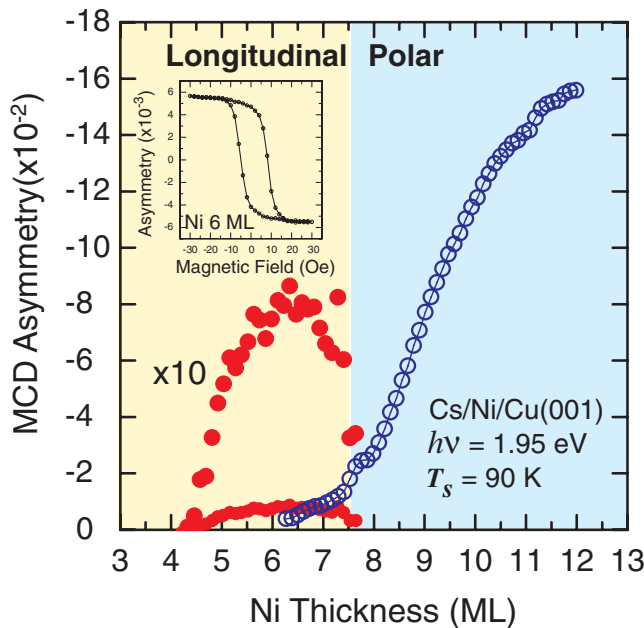


FIG. 2 (color online). The MCD asymmetry for a wedge shaped Ni film on Cu(001) at $T_s = 90$ K, $h\nu = 1.95$ eV, and $\Phi = 1.8$ eV. (inset) A magnetization curve by the photoemission MCD on a 6 ML Ni film with in-plane magnetization.

ensation may be overcome by using MLD, although we have not verified this hypothesis in the present work.

Perpendicularly magnetized films show intense MCD. Figure 3(a) shows the MCD asymmetry of Fe(3 ML)/Cu(001). The Fe film on Cu(001) with the thickness of less than 10 ML shows perpendicular magnetic anisotropy [18]. At the photoemission threshold, the MCD asymmetry using the 1.95 eV laser is as much as $\sim -4\%$, again exhibiting large MCD for the perpendicularly magnetized sample. The difference between the asymmetries obtained by the 1.95 and 3.81 eV lasers is more significant than the above Ni/Cu(001) case. This result indicates the pronounced effect of the Cs deposition in the 3 ML Fe film since the film thickness is much smaller and the Cs effect is hence greater. It is also noted that the MCD asymmetry changes its sign at $h\nu - \Phi \sim 0.2$ (eV) and then maintains nonzero positive values (more than 1%) up to ~ 2 eV. This is in clear contrast to the result of the 12 ML Ni film described above.

We have also examined fcc Co and bcc Fe films grown on Cu(001) as other examples of in-plane magnetized films. These MCD results are shown in Figs. 3(b) and 3(c). The MCD asymmetries observed are at most 0.12% in Fe/Cu(001) and 0.5% in Co/Cu(001). The asymmetries in the in-plane magnetized films are again found to be much smaller than the perpendicular magnetized cases in spite of their large thicknesses. The MCD asymmetry in Co(15 ML)/Cu(001) exhibits a negative sign and a minimum near the threshold. This observation is quite similar to the perpendicularly magnetized Ni case shown in Fig. 1(c), although the intensity is much weaker. In contrast,

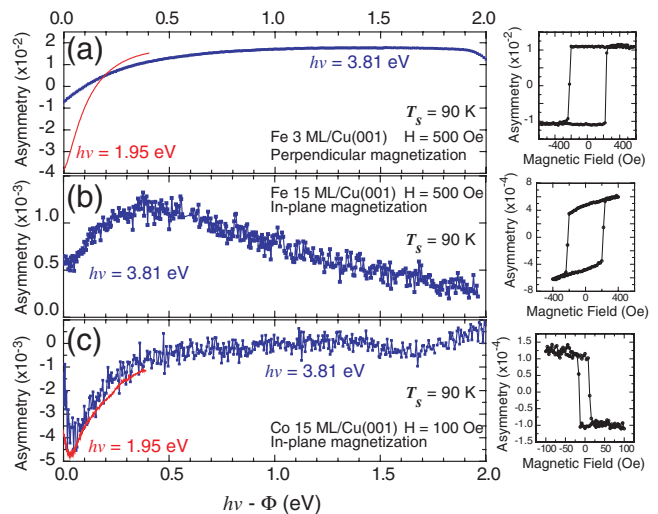


FIG. 3 (color online). MCD asymmetries on (a) a perpendicularly magnetized Cs/Fe(3 ML)/Cu(001) at normal incidence using the 3.81 and 1.95 eV lasers, (b) an in-plane magnetized Cs/Fe(15 ML)/Cu(001) with 30° incidence using the 3.81 eV laser, and (c) an in-plane magnetized Cs/Co(15 ML)/Cu(001). The right panels show corresponding magnetization curves for $\Phi \sim 1.8$ eV using the 1.95 eV laser.

Fe(15 ML)/Cu(001) shows different features. The MCD asymmetry is always positive and gives a broad maximum at $h\nu - \Phi \sim 0.4$ (eV).

Apart from the reflection of light, the MCD asymmetry basically depends on both the SOC and the spin polarization (exchange interaction). This is also the case for the Kerr rotation and ellipticity [6]. The MCD asymmetry is basically proportional to the magnitude of the SOC. Thus the observed large MCD asymmetries are partly ascribed to large orbital magnetic moments in ultrathin films. The present calculation, however, indicates that the abrupt drop of the calculated MCD asymmetry in Fig. 1(d) is associated with the change of the spin polarization in the integrated photoemission intensity and that the SOC does not change drastically in this narrow energy range around the threshold. On the other hand, near the threshold the photoelectrons along the surface normal [the ΓX direction in Ni(001)] are mainly probed, and it is experimentally known that the initial states for the threshold photoemission dominantly correspond to the minority band near the X point [10,19,20]. With increasing the energy $h\nu - \Phi$, the transition in the majority band should begin to take place, leading to a reduction of the spin polarization. Accordingly, the suppression and the sign reversal of the MCD asymmetry observed experimentally in the present work can be attributed mainly to the spin polarization.

Let us finally give a short discussion concerning the effect of Cs on the electronic structure. In Fig. 1(c), the two curves of the MCD asymmetry obtained by using the 3.81 eV and 1.95 eV lasers are not completely identical. The minimum energy positions differ by 0.03 eV from each other. The energy shift of the MCD peak indicates the electron donation from Cs to the Ni film [21]. The electron donation to the Ni films might result in more filling of the minority spin bands and the reduction of the exchange interaction. It should, however, be noted that the Cs effect is less important since the two curves of the MCD asymmetry do not differ so much. On the other hand, in the fcc Fe film in Fig. 3(a), the two curves of $h\nu = 1.95$ and 3.81 eV are more significantly different. This may be because the Fe film is much thinner than the Ni one, and the change of the electronic structure due to Cs deposition should be more important.

In conclusion, we have shown that the MCD asymmetry is substantially enhanced near the Fermi level. The perpendicularly magnetized 12 ML Ni film on Cu(001) provides as much as 10%–12% MCD asymmetry near the photoemission threshold. A large spin polarization near the Fermi level and a larger spin-orbit coupling in the ultrathin films than in the bulk give rise to the enhanced MCD. The present method does not require spin detectors or tunable synchrotron radiation x-ray sources. Considering such a large MCD asymmetry and a high brilliance of lasers,

PEEM experiments with short pulse lasers will pave new ways to the study of ultrafast dynamics in magnetization on surfaces and thin films.

We are grateful for the financial supports of Grant-in-Aid for Scientific Research (No. 15201029, No. 15087211, and No. 16710093) from Ministry of Education, Culture, Sports, Science, and Technology (MEXT), and SUMITOMO Foundation.

*Email address: yokoyama@ims.ac.jp

- [1] J. Stöhr, *J. Magn. Magn. Mater.* **200**, 470 (1999).
- [2] B. T. Thole, P. Carra, F. Sette, and G. van der Laan, *Phys. Rev. Lett.* **68**, 1943 (1992).
- [3] P. Carra, B. T. Thole, M. Altarelli, and X. Wang, *Phys. Rev. Lett.* **70**, 694 (1993).
- [4] J. Stöhr, Y. Wu, B. D. Hermsmeier, M. G. Samant, G. R. Harp, S. Koranda, D. Dunham, and B. P. Tonner, *Science* **259**, 658 (1993).
- [5] D. Neeb, A. Krasnyuk, A. Oelsner, S. A. Nepijko, H. J. Elmers, A. Kuksov, M. Bolte, C. M. Schneider, and G. Schönhense, *J. Phys. Condens. Matter* **17**, S1381 (2005).
- [6] H. Ebert, *Rep. Prog. Phys.* **59**, 1665 (1996).
- [7] Z. Q. Qiu and S. D. Bader, *Rev. Sci. Instrum.* **71**, 1243 (2000).
- [8] C. M. Schneider, M. S. Hammond, P. Schuster, A. Cebollada, R. Miranda, and J. Kirschner, *Phys. Rev. B* **44**, R12066 (1991).
- [9] W. Kuch, A. Dittschar, K. Meinel, M. Zharnikov, C. M. Schneider, J. Kirschner, J. Henk, and R. Feder, *Phys. Rev. B* **53**, 11 621 (1996).
- [10] W. Kuch and C. M. Schneider, *Rep. Prog. Phys.* **64**, 147 (2001).
- [11] G. K. L. Marx, H. J. Elmers, and G. Schönhense, *Phys. Rev. Lett.* **84**, 5888 (2000).
- [12] P. Blaha, K. Schwarz, G. K. H. Madsen, D. Kvasnicka, and J. Luitz, computer code WIEN2K, Technische Universität Wien, Vienna, 2002.
- [13] J. Kuneš, P. Novák, M. Diviš, and P. M. Oppeneer, *Phys. Rev. B* **63**, 205111 (2001).
- [14] P. M. Oppeneer, T. Maurer, J. Sticht, and J. Kubler, *Phys. Rev. B* **45**, 10 924 (1992).
- [15] B. Schulz and K. Baberschke, *Phys. Rev. B* **50**, 13 467 (1994).
- [16] J. Zak, E. R. Moog, C. Liu, and S. D. Bader, *Phys. Rev. B* **43**, 6423 (1991).
- [17] W. Kuch, J. Gilles, S. S. Kang, S. Imada, S. Suga, and J. Kirschner, *Phys. Rev. B* **62**, 3824 (2000).
- [18] J. Thomassen, F. May, B. Feldmann, M. Wuttig, and H. Ibach, *Phys. Rev. Lett.* **69**, 3831 (1992).
- [19] I. D. Moore and J. B. Pendry, *J. Phys. C* **11**, 4615 (1978).
- [20] J. Henk and B. Johansson, *J. Electron Specrosc. Relat. Phenom.* **94**, 259 (1998).
- [21] T. Nakagawa, H. Watanebe, and T. Yokoyama (to be published).